COMPUTER METHODS AND PROGRAMS IN BIOMEDICINE XXX (2015) XXX–XXX

journal homepage: www.intl.elsevierhealth.com/journals/cmpb

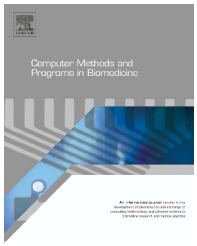

Non-invasive real-time prediction of inner knee temperatures during therapeutic cooling

Aleksandra Rashkovska[a,*], *Dragi Kocev*[b], *Roman Trobec*[a]

[a] *Department of Communication Systems, Jožef Stefan Institute, Jamova 39, 1000 Ljubljana, Slovenia*
[b] *Department of Knowledge Technologies, Jožef Stefan Institute, Jamova 39, 1000 Ljubljana, Slovenia*

ARTICLE INFO

Article history:
Received 11 February 2015
Received in revised form
16 June 2015
Accepted 6 July 2015

Keywords:
Biomedicine
Cryotherapy
Computer simulation
Predictive modeling
Feature ranking

ABSTRACT

The paper addresses the issue of non-invasive real-time prediction of hidden inner body temperature variables during therapeutic cooling or heating and proposes a solution that uses computer simulations and machine learning. The proposed approach is applied on a real-world problem in the domain of biomedicine – prediction of inner knee temperatures during therapeutic cooling (cryotherapy) after anterior cruciate ligament (ACL) reconstructive surgery. A validated simulation model of the cryotherapeutic treatment is used to generate a substantial amount of diverse data from different simulation scenarios. We apply machine learning methods on the simulated data to construct a predictive model that provides a prediction for the inner temperature variable based on other system variables whose measurement is more feasible, i.e. skin temperatures. First, we perform feature ranking using the RReliefF method. Next, based on the feature ranking results, we investigate the predictive performance and time/memory efficiency of several predictive modeling methods: linear regression, regression trees, model trees, and ensembles of regression and model trees. Results have shown that using only temperatures from skin sensors as input attributes gives excellent prediction for the temperature in the knee center. Moreover, satisfying predictive accuracy is also achieved using short history of temperatures from just two skin sensors (placed anterior and posterior to the knee) as input variables. The model trees perform the best with prediction error in the same range as the accuracy of the simulated data (0.1 °C). Furthermore, they satisfy the requirements for small memory size and real-time response. We successfully validate the best performing model tree with real data from in vivo temperature measurement from a patient undergoing cryotherapy after ACL reconstruction.

1. Introduction

Measurements in biomedicine are often difficult to perform because human subjects are involved. Many examples can be found, particularly in clinical procedures, where in vivo measurements are often not as accurate as desired [3], difficult, dangerous or even impossible to perform [46], especially if deep tissues or vital organs are in question [15,38]. Moreover, non-invasive medical procedures are emerging in the search for more reliable, less expensive, and risk-free medical technology for the future [31,34,40].

Computer simulations provide safe and inexpensive insight into physiological processes. In recent decades, computer simulations have significantly helped to better

* *Corresponding author*. Tel.: +386 1 477 3701; fax: +386 1 477 3111.
E-mail address: Aleksandra.Rashkovska@ijs.si (A. Rashkovska) .

http://dx.doi.org/10.1016/j.cmpb.2015.07.004
0169-2607/

understand and solve a variety of problems in science. Advances in computer technology enable simulation of natural phenomena that cannot be subject to experiments in reality because of ecological, hazardous or financial obstructions [18]. With the use of computer simulation, it is possible to calculate, analyze, and visualize both stationary and time-dependent temperature fields in living biological tissues [11]. The temperature of the human tissue is an important factor in many fields of physiology [51], sports [14], cryotherapy [19], etc.

In the context of the issues addressed above, computer simulations can be useful to estimate an immeasurable variable or a variable difficult to be measured based on other variables of the system/process whose measurement is more feasible – a concept known as soft or virtual sensing [2]. In the case of biomedical systems, if the variable of interest cannot be measured because of the non-invasive nature of the system – hidden system variable, then we should measure other non-invasive variables that can be used to estimate the hidden one. However, simulations are usually resource- and time-consuming which is not acceptable in real-time systems [42]. We assume that real-time biomedical systems, for example, for the purpose of controlling the variable of interest, require a solution usually deployed on a mini on-board computer that cannot process large amount of data nor perform computationally demanding operations.

To this end, we use machine learning methods [20] to construct a predictive model that will provide a prediction for the hidden variable in a much shorter time with satisfying accuracy. Namely, we use simulation to generate a substantial amount of data for different input simulation parameters: capture the correlation between the hidden system variable and the non-invasive measurable ones. The data generated in this way is then used to construct a predictive model. There are two main advantages of using predictive models: (1) a predictive model can be used to simplify the simulation model and elucidate the most important correlations between the measurable (input) variables and non-measurable (output) variables, and (2) the predictive models are typically more efficient in terms of memory and computational complexity. Various machine learning techniques have proven to be adequate for extracting knowledge from data resulting from simulation models in various areas like medicine [5,10], ecology [9], social sciences [21], etc.

In this paper, we apply this approach on a real-world problem in the domain of biomedicine – non-invasive real-time prediction of inner knee temperature during cryotherapeutic treatment after anterior cruciate ligament (ACL) reconstructive surgery of a knee. It is known, mostly from empirical evidence, that cryotherapy following reconstruction contributes to reduced tissue edema, inflammation, hematoma formation and pain, reducing the need for pain medication and enabling faster rehabilitation [35]. Various cooling modalities are routinely used in postoperative treatment in orthopedics, traumatology, facial surgery, pain prevention in sport [11], etc. In a previous study, we have shown that computer-controlled cryotherapy with pre-programmed protocols in terms of heat extraction intensity and treatment time is more effective and controllable than a conventional cooling with gel-packs [29]. We measured in vivo temperatures of the inner and outer knee parts and assessed the effectiveness of both methods. Moreover, we confirmed delayed and less severe pain in patients with the computer-controlled cryotherapy. However, a lack of uniformity in patients' response to the cooling was confirmed, which raised the need for "smart" cooling devices, i.e. personalized cryotherapy. Different patients need different cooling protocols, depending on their constitution and regulatory systems, and on environmental conditions. A "smart" cooling device would be able to perform cooling adapted to the individual patient's response. Therefore, we propose an upgrade of the method for computer-controlled cryotherapy by introducing automatic control of the temperature inside the knee by changing the cooling temperature in the pad [28]. A few non-invasive temperature sensors on the knee surface, providing data about the actual heat transfer and the physiological response of the patient, should give a feedback for the process of control. To control the deep knee temperature successfully in an arbitrary knee without measuring it, we need to estimate the deep temperature from the non-invasively measured data using predictive models – the main goal of this paper. The light-weighted predictive models will then correspond to the mini architecture of the computer that controls the cryotherapy. Our previous work in the field of heat transfer in biological tissues forms the ground base for providing the simulated data [30].

The machine learning tasks that we address in this paper belong to the predictive modeling setting where the goal is to predict the value of one property of the examples (called a target attribute or output) using the values of the remaining properties (called descriptive or input attributes) [17]. Considering that the solution requires efficient predictive models, we investigate and evaluate several state-of-the-art machine learning methods. The machine learning methods that we will consider include simple methods, such as linear regression and regression trees, as well as more complex methods, such as model trees, and ensembles of regression and model trees. The simple methods will also provide efficient and understandable predictive models, i.e., with these models we will be able to infer the most important correlations between the input and output variables. The complex methods, on the other hand, will be black-box models and will offer state-of-the-art predictive power. The methods will be evaluated based on the predictive power and the time/memory efficiency of the models they construct. At the end, we will select the best performing method that can be further used, for example, for control of the hidden output variable in real-time. Moreover, we validate the best performing method with real data from in vivo temperature measurement from a patient undergoing cryotherapy after ACL reconstruction. Furthermore, we use methods for feature ranking to provide an ordered list of the input variables by their relevance or importance for the output/target variable [16]. We use these methods to investigate which input variables are sufficient for making a good prediction and to which extent we need to measure them in time. The expected benefit would be the reduction of the number of sensors and construction of even smaller and more efficient predictive models.

The rest of the paper is organized as follows. In Section 2, we present the background knowledge from computer

Please cite this article in press as: A. Rashkovska, et al., Non-invasive real-time prediction of inner knee temperatures during therapeutic cooling, Comput. Methods Programs Biomed. (2015), http://dx.doi.org/10.1016/j.cmpb.2015.07.004

simulations of topical cooling and the design of the simulation scenarios in order to generate the data set for the machine learning tasks. The simulation model has been previously validated on a set of measurements from therapeutic knee cooling [42,45]. Next, in Section 3, we present the machine learning tasks considered – feature ranking and predictive modeling methods. In Section 4, the results from feature ranking, and the evaluation of the predictive performance and time/memory efficiency of the constructed predictive models, are presented and discussed. Finally, the paper concludes with a summary of the results and directions for further work in Section 5.

2. Computer simulation of therapeutic knee cooling

In this section, we first present the computer simulation model for therapeutic knee cooling. After that, we give the settings for various simulation scenarios used to generate a large amount of data for the machine learning tasks.

2.1. Simulation model

In computer simulations, a physical system is represented by a mathematical model that cannot be solved analytically. Thus, an adequate numerical approach is required to obtain the numerical solution [13]. For this purpose, the continuous physical domain is replaced by its discrete form, usually by imposing a grid and partitioning the physical domain into many small sub-domains. Solving the mathematical model over discretized domain gives the value of a certain physical quantity at every grid point for each time interval. In the majority of simulations, the classical numerical methods, such as the Finite Difference Method (FDM) or the Finite Element Method (FEM) [42], are used.

In this paper, the interest is in computer simulations of heat transfer in biological tissues. The basis of the simulation model for heat transfer in biological tissues is the well-known Pennes' Bio-heat equation that incorporates classical heat transport and the heat generated from the biological response of the tissues, i.e., the heat transfer between the arterial blood and the tissues, and the heat production by tissue metabolism [26,48]:

$$\frac{\partial T}{\partial t} = \underbrace{\frac{1}{\rho c_p}\nabla\cdot(\lambda\nabla T)}_{\text{heat transport}} + \overbrace{\underbrace{\frac{\rho^b c_p^b}{\rho c_p} V_r(T)(T_a - T)}_{\text{blood perfusion}} + \underbrace{\frac{1}{c_p} h_m(T)}_{\text{metabolic heat production}}}^{\text{biological response}}, \quad (1)$$

where $\nabla = (\partial/\partial x, \partial/\partial y, \partial/\partial z)$ is differential operator in terms of Cartesian coordinates (x, y, z), T is the temperature of a tissue, t is time, ρ, c_p and λ are density, specific heat, and thermal conductivity of a tissue, ρ^b and c_p^b are density and specific heat of the blood. The function $V_r(T)$ is the blood flow rate and the function $h_m(T)$ is the metabolic heat production per unit mass. The temperature $T_a = 36.8\,^\circ$C stands for the reference tissue temperature.

The total blood flow is separated into regional blood flows $V_r(T)$ for each tissue:

$$V_r(T) = v_r V(T). \quad (2)$$

The regional blood flow rate $V_r(T)$ is modeled with the exponential function $V(T_s)$ multiplied with dimensionless regional blood flow rate fraction v_r [43]:

$$V(T_s) = (5.142 \cdot 10^{-5} e^{0.322 T_s} + 0.705)\,\text{ml}\,(100\,\text{ml})^{-1}\text{min}^{-1}, \quad (3)$$

where T_s is the skin temperature. The fraction v_r is introduced to enable different blood flow rates in different tissues and it was not included in the original Pennes' equation. The v_r values for different tissues were determined based on measured ratios between blood flow rates in different tissues [39] using an iterative procedure while maintaining the mean blood flow rate [43].

The rate of metabolic heat production per unit mass h_m is assumed to obey the Q10 rule [41], which is expressed as a function of the tissue temperature:

$$h_m(T) = h_r 2^{(T-T_r)/10}, \quad (4)$$

where h_r stands for the reference metabolic heat production of a tissue at reference temperature $T_r = 35^\circ$C. For muscles at rest, h_r was taken to be about half the human basal metabolic rate, which equals 0.6 W/kg [37].

The heat flow between the skin surface and the ambient air is simulated using convective boundary conditions [4], based on the continuity of the heat flow perpendicular to the surface of the simulated body part:

$$\lambda\frac{\partial T}{\partial n} = H(T_{am} - T), \quad (5)$$

where T_{am} stands for the ambient temperature. The convection coefficient $H = 16\,\text{Wm}^2/^\circ\text{C}$ is determined by numerical experiments, based on simulation of the thermo-neutral conditions ($T_{am} = 26\,^\circ$C and $T_s = 33\,^\circ$C) [43], maintained also by Pennes' measurements. $\partial/\partial n$ denotes derivative along the outward normal to the face of the surface voxel in contact with the air.

Outside biological tissues, the Bio-heat equation is reduced to diffusion equation as both additional source terms (heat transfer between blood and tissues, and metabolism) vanish. No flow is allowed in the tissue and only incompressible fluids are considered. A substantial amount of work on closed form and numerical solutions of the Bio-heat equation has been published [4,8,22–24,26,50]. Our previous work in this field includes computer simulation of heat transfer in different body parts [30]. Spatial models of human body parts, in particular, a human heart [38,46], knee [45] and forearm [43], along with parallel programs for simulation of their cooling during and after surgery, have been developed.

The paper concerns the simulation of topical cooling (cryotherapy) of a human knee after ACL reconstructive surgery. The computational domain of the simulation is composed of the knee model and surrounding layers: protective bandage, cooling layer, isolating blanket and ambient air. The

Please cite this article in press as: A. Rashkovska, et al., Non-invasive real-time prediction of inner knee temperatures during therapeutic cooling, Comput. Methods Programs Biomed. (2015), http://dx.doi.org/10.1016/j.cmpb.2015.07.004

knee is modeled as a 3D closed cavity. The model is obtained through expert assisted segmentation of human body parts from the Visible Human Dataset (VHD) [1]. The body parts are composed of different tissues (muscles, bones, cartilage, fat, vessels and nerves). Considering the complexity of the modeled body part, spatial dependent thermo-physical properties are employed. The final geometric domain is composed of small cubic voxels, resulting in millions of discretization points.

The initial conditions of the simulation comprise the initial temperatures of the modeled tissues. The temperature of the blood in the artery is set to a constant value of 36.8 °C with Dirichlet boundary conditions on the artery walls, assuming well-mixed blood with a significant flow. Moving air is not simulated because of its significant contribution to the calculation complexity [44]. The ambient air is assumed to be well-mixed and thus has a constant temperature. The heat flux from the first and last slices is kept constant in order to imitate the influence of the leg not exposed to the cooling. Simulations are performed on the described model using realistic process parameters gathered from measurements (Table 1).

The governing system of PDEs is numerically solved on parallel computers using the Explicit Finite Difference Method (EFDM) [25]. It is a simple implementation of a numerical scheme for inhomogeneous tissue with low calculation complexity and straightforward parallelization. Using FDM, the geometric domain is first discretized in space with a rectangular mesh of points with four neighbors in 2D or with six neighbors in 3D. The spatial derivatives in the mathematical model are replaced by finite differences. An equation is formed for each voxel using collocation, which states that the model equations should be satisfied exactly at all points. After spatial discretization, the PDEs are transformed into a system of ordinary differential equations (ODEs) that can be solved using time discretization. The time discretization method used is the explicit Euler's method, because the approximate solution value in the next time-step is obtained from already known solutions in the previous time-step. The explicit methods are simple and require just matrix-vector multiplication at each time-step, while implicit methods require solution of a system of equations at each time-step in order to proceed to the next simulation time-step. Thus, by approximating the time derivatives with finite differences, a system of algebraic equations is obtained, which can be solved analytically. Starting with the initial condition and stepping in time, we can get the approximate solution of the system for each voxel at any time step.

The method described has several limitations. Spatial models differ with different persons and with time, and consequently the simulated results can differ. Minor errors in tissue segmentation and inaccurate thermodynamic constants could also produce small errors in the simulated results. Personal regulatory mechanisms have not been included in the simulation model but could easily be incorporated. All such limitations could have some impact on the simulated temperatures; however, previous validations of the simulation model for different cooling or heating methods of different body parts have confirmed that the used model and numerical procedure are appropriate for simulation of heat transfer in bio-tissues [30,43,45]. For example, in Fig. 1, the simulated steady-state temperature profile for a naked knee and the temperature profile after 90 min of simulated cooling at 9 °C are shown for the model slice z = 101 along the y

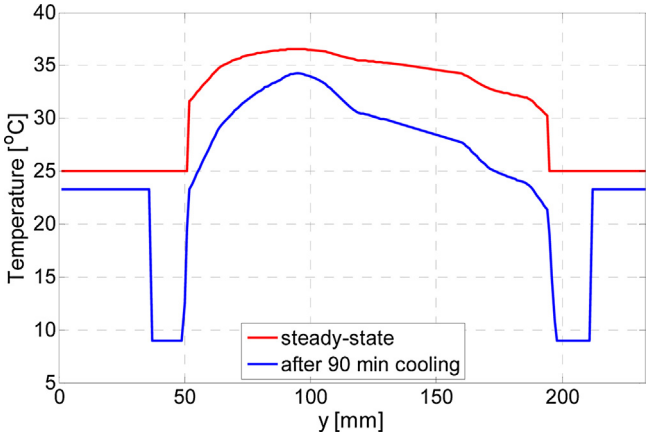

Fig. 1 – Steady-state temperature profile for a naked knee and temperature profile after 90 min of cooling at 9 °C for the model slice z = 101 along the y axis for x = 105.

Table 1 – Thermo-physical parameters and initial temperatures of simulated substances. Constant temperatures are denoted by (*).

Substance	λ [W/mK]	c_p [J/kg K]	ρ [kg/m^3]	v_r	h_r [W/kg]	T [°C]
Skin	0.51	3431	1200	0.4	0.3725	35
Subcutaneous tissue	0.55	2241	812	0.4	0.3725	35.6
Muscle	1.03	4668	1179	0.8	0.6573	36
Bone	2.28	1260	1700	0.2	0.0372	36
Ligament	0.33	3966	1250	0.2	0.0372	36
Cartilage	1.5	2275	1160	0.2	0.0372	36
Nerve	0.5	3277	1190	1.1	0.3725	36
Venous blood	0.67	3890	1057	0	0.0372	36
Arterial blood	0.67	3890	1057	0	0.0372	36.8*
Meniscus	1.5	2275	1160	0.2	0.0372	36
Joint liquid	0.58	4204	1000	0	0	22
Ambient air	0.025	1012	1.29	0	0	25*
Bandage	0.04	1175	150	0	0	30
Blanket	0.05	1200	450	0	0	25
Cooling liquid	0.58	4204	1000	0	0	9*

Please cite this article in press as: A. Rashkovska, et al., Non-invasive real-time prediction of inner knee temperatures during therapeutic cooling, Comput. Methods Programs Biomed. (2015), http://dx.doi.org/10.1016/j.cmpb.2015.07.004

(anteroposterior) axis for x = 105 (the center of the knee, i.e. in the intercondylar notch). The figure shows that the gradients in the temperature profiles after cooling are much more pronounced compared to the steady-state.

2.2. Simulations design

Computer simulation data of human knee temperatures during cooling after surgery provides the basis for the predictive modeling tasks. A substantial amount of diverse data is needed for the predictive model to capture the relation between the inner knee temperatures and the outer knee temperatures with satisfying accuracy for a wide range of human knees and cooling settings. Therefore, using the presented simulation model, the simulation data is generated from different simulation scenarios with variation of the simulation parameters. Previous evaluations [30] have shown that variations in the knee dimension and the blood flow rate have the most important impact on the temperature profiles. Moreover, analyses showed that the difference between the simulations in 3D and in 2D under the same conditions is not significant. We have thus performed 2D computer simulation of two hours of knee cooling after surgery for 1400 different settings resulting from:

- 10 knee dimension settings, starting from normal knee dimension and then scaling down to a small knee and up to a big knee. The variations in knee dimension were set in the range of real-value human knee dimensions.
- 10 blood flow rate settings, starting from normal blood flow rate with the blood flow parameters for different tissues set as in Table 1, and then scaling linearly up and down by 20%.
- 14 cooling temperatures ranging from 2 °C to 15 °C. The range and the accuracy of 1 °C for the cooling temperature was set according to the specifications of today's cryotherapeutic devices, namely, the CTS100 by Waegener [47].

Simulation of arthroscopic surgery and resting after surgery, starting from steady-state, preceded the simulation of cooling for each setting. The model slice 101 from the central knee region was taken as computational domain in 2D. For each setting, the temperature distribution for the whole computational domain was saved for two hours every second (7200 s) with an accuracy of 0.1 °C. The data resulting from the simulation totaled $10 \times 10 \times 14 \times 7200 = 10{,}080{,}000$ temperature distribution files. Each file had size of approximately 1 MB, which resulted in approximately 10 TB of raw simulation data. This data was further processed to obtain the dataset for the tasks of predictive modeling.

3. Machine learning tasks

In this section, we first describe the pre-processing of the simulation results to obtain the dataset for the machine learning tasks. Next, we present the two machine learning tasks used to analyze the data: we first present the RReliefF feature ranking algorithm and then overview several methods for learning regression predictive models.

3.1. Data pre-processing

The main machine learning task considered here belongs to the predictive modeling setting, i.e., building a predictive model that will predict the inner knee temperature as output or target attribute based on other outer knee temperatures as descriptive or input attributes. The simulated raw data was pre-processed to obtain the dataset for the predictive modeling tasks. The positions of the voxels whose temperature was extracted as input and output attributes are schematically shown in Fig. 2 on the geometric model of the knee used in the simulation.

The input temperature attributes are temperatures on four locations on the knee skin (SK1, SK2, SK3, SK4), and on four respective locations on the protective bandage (BA1, BA2, BA3, BA4). The output temperature is the temperature in the intercondylar notch (ICN). Furthermore, the knee dimension (KD) and the temperature of the cooling liquid (CT) are also considered as input attributes. The dataset also includes a short history of each input temperature attribute: the values of the temperature attributes are all taken in the current and in five previous time steps with the resolution of 1 s, meaning that the data extracted from a temperature distribution file are accompanied with data extracted from five previous temperature distribution files. The notations of the input temperature attributes for the training dataset are given in Table 2.

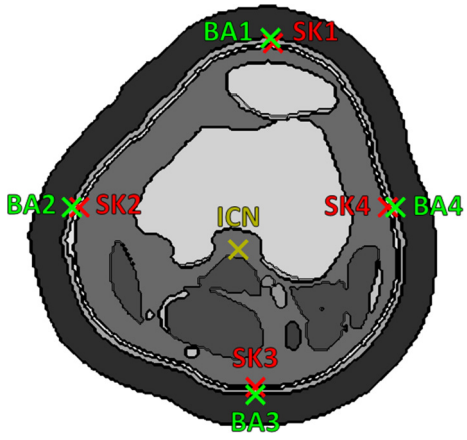

Fig. 2 – Positions of inner and outer knee voxels whose temperatures are used in the training dataset. The positions are marked with crosses on knee model slice 101 in the level of the intercondylar notch. ICN – intercondylar notch, SK – skin, BA – bandage (1 – anterior, 2 – medial, 3 – posterior, 4 – lateral).

Table 2 – Notation of the input temperature attributes. SK – skin, BA – bandage (1 – anterior, 2 – medial, 3 – posterior, 4 – lateral).

Time (s)	SK1	SK2	SK3	SK4	BA1	BA2	BA3	BA4
−0	SK1_0	SK2_0	SK3_0	SK4_0	BA1_0	BA2_0	BA3_0	BA4_0
−1	SK1_1	SK2_1	SK3_1	SK4_1	BA1_1	BA2_1	BA3_1	BA4_1
−2	SK1_2	SK2_2	SK3_2	SK4_2	BA1_2	BA2_2	BA3_2	BA4_2
−3	SK1_3	SK2_3	SK3_3	SK4_3	BA1_3	BA2_3	BA3_3	BA4_3
−4	SK1_4	SK2_4	SK3_4	SK4_4	BA1_4	BA2_4	BA3_4	BA4_4
−5	SK1_5	SK2_5	SK3_5	SK4_5	BA1_5	BA2_5	BA3_5	BA4_5

Please cite this article in press as: A. Rashkovska, et al., Non-invasive real-time prediction of inner knee temperatures during therapeutic cooling, Comput. Methods Programs Biomed. (2015), http://dx.doi.org/10.1016/j.cmpb.2015.07.004

An instance for the resulting dataset was extracted from each of the 10,080,000 temperature distribution files. The dataset was further checked for duplicate instances and they were excluded from further analysis because such samples could influence the distribution of the target variable and hence disturb the learning of the predictive model. The preprocessing resulted in downsize of the data from around 10 TB raw simulation data to 591 MB large dataset.

3.2. *Feature ranking with RReliefF*

The first task performed on the dataset is feature ranking using the RReliefF algorithm [32]. The major competitive advantage of the Relief family of algorithms (including RReliefF), compared to other methods for estimating the importance of features, is that they are able to capture the relevance for features involved in feature interactions [33]. Moreover, these algorithms are efficient, aware of the contextual information, and able to correctly estimate the variable relevance in domains that contain strong dependencies between the variables.

The RReliefF algorithm begins with a random selection of an example from the training data. Next, it looks for its k-nearest neighbors and calculates the importance of each attribute. The importance is calculated using a probabilistic definition about the distance between the predicted values. Moreover, the neighbors closer to the selected example influence more on the overall score than the ones that are more distant (exponentially decreasing influence defined with the exponent *sigma parameter* of the algorithm).

The RReliefF algorithm has two parameters that need to be instantiated depending on the application domain: sample size and number of nearest neighbors. The number of randomly selected examples (sample size), used to estimate the importance of the features, corresponds to the *iterations parameter* of the algorithm (as called within the WEKA [49] tool). In Ref. [33], it is shown that the estimates of attributes' importance stabilize relatively fast, i.e., after only several tens of iterations; nonetheless, this value is application dependent. The second parameter of the RReliefF algorithm is the number of nearest neighbors considered for the estimates of the attributes importance. This parameter controls the amount of local or global information that the algorithm exploits. The RReliefF algorithm is relatively robust to the number of nearest neighbors as long as this number remains relatively small compared to the sample size.

For selecting the proper parameter values for the algorithm, we have employed the recommendations given in Ref. [33]. For the sample size, i.e. the *iteration parameter* of the algorithm, we have set the value to 1000 examples. We have also performed experiments with smaller and larger sample sizes; however, the results were quite similar to each other, which indicates that the estimates of attributes' importance are stable. For the number of nearest neighbors, we have set the value to 70 neighbors with exponentially decreasing influence (the value of the *sigma parameter* was set to 20).

To further obtain more stable results, we use 10-fold cross-validation. This procedure in the context of feature ranking is as follows. First, the training dataset is randomly partitioned into 10 subsets with equal size (each subset does not contain parts from the other subsets). Next, using 9 of the subsets, a new training dataset is constructed. This is repeated for 10 times, each time leaving one subset aside. On each of the 10 new training datasets, a feature ranking is then performed; thus, yielding 10 feature rankings. Finally, the estimates of attributes' importance and the ranks of the features are averaged across the 10 new training datasets and they are reported as average merit and average rank, together with the respective standard deviation.

3.3. *Predictive modeling*

The second machine learning task is the learning of predictive models based on specific scenarios (datasets from a subset of input attributes) regarding the feature ranking results. For each of the defined scenarios, we evaluate the performance of several methods for predictive modeling: linear regression, regression trees and model trees for different pruning parameters (i.e., variation of the minimal number of examples per leaf), and ensembles of regression and model trees. We briefly present these methods and the evaluation methodology in the remainder of this section.

Linear regression is one of the simplest methods for solving regression tasks and it has been used for decades. The main rationale behind this method is to calculate the target variable as a linear combination of the descriptive attributes using weights that are calculated on the training dataset. Although linear regression is a very simple and efficient method, the produced models suffer from the fact that they look for linear relations that possibly exist in the data [49]. However, the data in a large majority of real-life applications exhibit some nonlinarites. Thus, the linear model with the best-fitted straight line (best in the sense of least squared difference) may not fit very well on the data. Nonetheless, these models can be used as components of more complex methods, such as model trees.

Regression and model trees are very similar predictive models. Both regression and model trees are decision trees for predicting the value of a continuous/numeric target variable [7]. Regression and model trees are hierarchical structures where the internal nodes contain tests on the input attributes. Each branch of an internal test corresponds to an outcome of the test, and the prediction for the value of the target attribute is stored in a leaf. The only difference between regression and model trees is how they calculate the prediction. Namely, leafs of a regression tree contain constant values as predictions for the target variable; therefore, a regression tree represents a piece-wise constant function. On the other hand, leafs of a model tree contain a linear function calculated using the examples belonging to the given leaf [27]; hence, a model tree represents a piece-wise linear function. In this paper, we use the M5P implementation of these models from the WEKA machine learning tool. The tree construction algorithm belongs to the group of greedy divide-and-conquer algorithms. The construction algorithm is known as Top-Down Induction of Decision Trees (TDIDT).

After a regression/model tree is constructed, it is common to prune it in order to improve its predictive power and interpretability [12]. The pruning protects against over-fitting the constructed trees to the training data at hand and improves

Please cite this article in press as: A. Rashkovska, et al., Non-invasive real-time prediction of inner knee temperatures during therapeutic cooling, Comput. Methods Programs Biomed. (2015), http://dx.doi.org/10.1016/j.cmpb.2015.07.004

the predictive performance on unseen examples. The pruning methods are typically integrated into the tree construction algorithm as stopping criteria and they are called pre-pruning methods.

The predictive performance of the regression and model trees can be further improved if they are combined into an ensemble [6]. An ensemble is a set of base predictive models whose predictions are combined to obtain an overall prediction. The performance of the ensembles is better if the base predictive models have good predictive performance and are different among each other. Most famous ensemble methods for tree-based predictive models are bagging, random forests and boosting [36], with bagging being the most widely used method. Bagging constructs its base predictive models using bootstrap replicates of the training data. To produce a prediction for an example, the ensemble sorts the example through each base predictive model and the overall prediction is obtained by averaging the predictions of the base predictive models.

Considering that the solution requires efficient predictive models that perform in real-time, the methods are evaluated based on the time/memory efficiency of the models they construct and their predictive performance. The models' time efficiency is measured as time needed to produce a prediction for a new instance, and the models' memory efficiency is measured as the size of the model file produced by the WEKA modeling suite (note that this size is related also to the model size in terms of tree nodes and/or equation terms). Given the design request for the models to perform real-time on a small on-board computer (with limited memory and computing power), we will aim to select models that have fast response and are light-weighted.

As measures for the models' predictive performance, we used correlation coefficient (CC) and mean absolute error (MAE) between the real and the predicted values of the target variable. The predictive performance of a predictive model is the estimation of the models' performance on new and previously unseen examples. Typically, the predictive performance is estimated using hold-out testing set of examples or by using k-fold cross validation (i.e., its most famous variant – 10-fold cross validation). The latter is a standard statistical procedure for performance estimation widely used by the machine learning research community and also in the paper. This procedure in the context of predictive modeling is as follows. First, the original dataset is randomly partitioned into 10 equal-size subsets. Next, a single subset is retained for validation of the model, and the remaining 9 subsets are used as training data. The cross-validation process is then repeated 10 times (the folds), with each of the 10 subsets used exactly once as validation data. Finally, the 10 results from each fold are averaged (or otherwise combined) to produce a single estimation.

4. Results and discussion

This section presents and discusses the results for real-time prediction of inner knee temperature during therapeutic cooling. First, the feature ranking results are presented and discussed. Next, considering the results from feature ranking, we define predictive modeling scenarios to be investigated. The predictive modeling results are presented and discussed based on the predictive performance and time/memory efficiency of the constructed predictive models.

4.1. *Feature ranking results*

The results of feature ranking with the RReliefF algorithm are given in Table 3. The descriptive variables in the table are ordered by the *average rank* of the attributes from the 10-fold cross-validation procedure. The relatively low values for the *average merit* of the importance estimates are due to the specific domain. Namely, the examples in this domain are very close to each other, thus the values for the target variable of the selected nearest neighbors by RReliefF are also close to each other. Therefore, the attributes receive lower values for the estimate of their importance. Nevertheless, the results give valid indications about the attributes' importance.

Table 3 – Results from the feature ranking with RReliefF. The notations of the input temperature attributes are given in Table 2. Additional notations: KD – knee dimension, CT – cooling temperature.

Attribute	Average rank	Average merit	Attribute	Average rank	Average merit	Attribute	Average rank	Average merit
SK1_0	1.9 ± 1.22	0.002 ± 0.001	SK2_1	17.9 ± 2.88	0.001 ± 0	BA2_0	34.2 ± 7.08	0 ± 0
SK1_5	2.6 ± 1.43	0.002 ± 0	SK2_4	20.4 ± 2.42	0 ± 0	BA3_1	36.1 ± 3.62	0 ± 0
SK1_4	3.8 ± 1.33	0.002 ± 0	SK4_4	21.3 ± 1.90	0 ± 0	BA3_4	36.8 ± 2.18	0 ± 0
SK3_0	3.9 ± 1.92	0.002 ± 0.001	SK4_1	21.4 ± 4.52	0 ± 0	BA3_3	38.0 ± 1.67	0 ± 0
SK1_3	5.0 ± 1.55	0.002 ± 0	SK2_2	21.8 ± 2.64	0 ± 0	BA3_2	39.1 ± 2.55	0 ± 0
SK1_1	6.1 ± 1.81	0.002 ± 0	SK2_3	23.3 ± 2.65	0 ± 0	BA4_5	39.6 ± 3.75	0 ± 0
SK1_2	6.3 ± 1.19	0.002 ± 0	SK4_3	23.6 ± 1.62	0 ± 0	CT	40.4 ± 6.33	0 ± 0
SK3_1	8.3 ± 2.37	0.002 ± 0	BA1_0	23.8 ± 4.21	0 ± 0	BA2_5	41.8 ± 1.4	0 ± 0
SK3_5	9.7 ± 1.19	0.002 ± 0	SK4_2	24.5 ± 1.43	0 ± 0	BA4_4	43.2 ± 2.56	0 ± 0
SK3_2	11.5 ± 1.2	0.002 ± 0	BA1_5	27.5 ± 1.28	0 ± 0	BA2_1	43.5 ± 5.08	0 ± 0
SK3_4	11.8 ± 1.47	0.002 ± 0	BA3_0	29.3 ± 4.12	0 ± 0	BA2_4	44.5 ± 1.91	0 ± 0
SK2_0	12.1 ± 3.59	0.001 ± 0.001	BA1_4	29.6 ± 1.74	0 ± 0	BA4_1	45.1 ± 4.68	0 ± 0
SK3_3	12.3 ± 0.9	0.001 ± 0	BA1_2	31.2 ± 1.99	0 ± 0	BA4_2	46.9 ± 1.92	0 ± 0
SK4_0	12.6 ± 4.22	0.001 ± 0.001	BA1_1	31.4 ± 3.01	0 ± 0	BA4_3	47.1 ± 1.97	0 ± 0
KD	15.3 ± 3.95	0.001 ± 0	BA1_3	31.9 ± 1.14	0 ± 0	BA2_2	47.3 ± 2.41	0 ± 0
SK4_5	16.4 ± 1.11	0.001 ± 0	BA4_0	34.2 ± 5.88	0 ± 0	BA2_3	47.9 ± 2.43	0 ± 0
SK2_5	16.6 ± 1.85	0.001 ± 0	BA3_5	34.2 ± 3.49	0 ± 0			

Please cite this article in press as: A. Rashkovska, et al., Non-invasive real-time prediction of inner knee temperatures during therapeutic cooling, Comput. Methods Programs Biomed. (2015), http://dx.doi.org/10.1016/j.cmpb.2015.07.004

The feature ranking results indicate that the SK temperatures are more relevant, especially SK1 and SK3 temperatures that correspond to the temperatures of skin sensors placed anterior and posterior to the knee. These findings can be explained by considering the anatomy of the knee, visible from the geometric model in Fig. 2. The knee anatomy is such that the anterior part of the knee consists mostly of bone that has the largest thermal conductivity from all tissues according to Table 1. Consequently, this part of the knee is most sensible to temperature changes. On the other hand, the posterior part of the knee is the one closer to the knee artery that acts as a constant heat source. Moreover, this part of the knee consists mostly of muscles with small thermal conductivity and therefore is the least sensible to temperature changes. This also explains the result that the history of SK1 temperature is more relevant than the SK3 temperature history. However, the posterior part of the knee is also relevant for indicating the ICN temperature because the ICN is located in the vicinity of the knee artery. Finally, the results indicate that the temperatures on the bandage are not relevant.

4.2. *Predictive modeling results*

Considering the feature ranking results, we define scenarios to be investigated and evaluated for their predictive performance and time/memory efficiency when modeling with linear regression, regression trees and model trees for different pruning parameters, and ensembles of regression and model trees. The predictive performance measures (CC and MAE) are presented with corresponding confidence intervals

Table 4 – Predictive modeling scenarios. The notations of the input temperature attributes are given in Table 2. Additional notations: KD – knee dimension, CT – cooling temperature, TNI – training number of instances.

Scenario	Input attributes	TNI
SC1	KD, CT, SK1_[0–5], SK2_[0–5], SK3_[0–5], SK4_[0–5]	1,930,028
SC2	KD, CT, SK1_0, SK2_0, SK3_0, SK4_0	510,399
SC3	KD, CT, SK1_[0–5], SK3_[0–5]	1,201,962
SC4	KD, CT, SK1_0, SK3_0	299,940
SC5	KD, CT, SK1_[0–5], SK3_[0–5], BA1_[0–5]	1,279,108

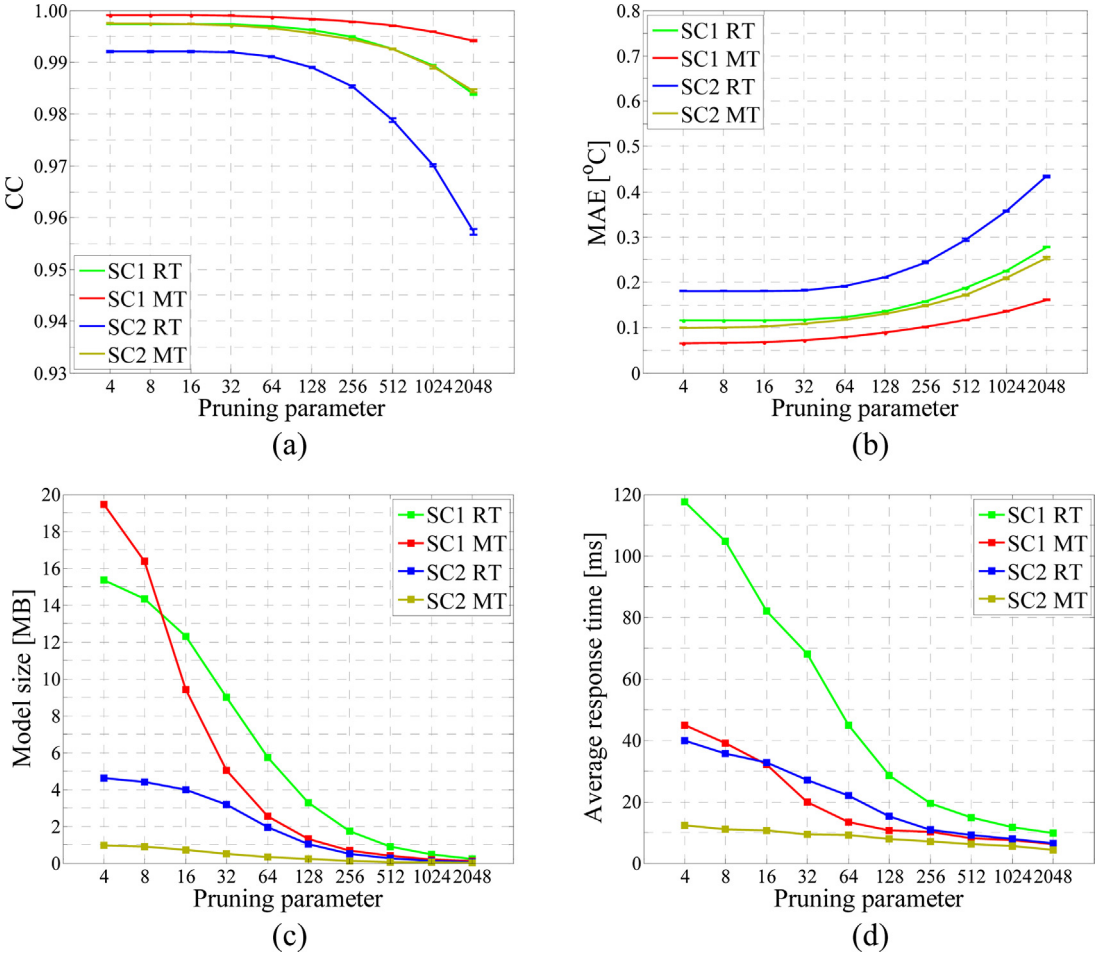

Fig. 3 – Performance of regression trees (RT) and model trees (MT) for SC1 and SC2 (a) correlation coefficient (CC), (b) mean absolute error (MAE), (c) model size and (d) time efficiency. SC1 and SC2 are defined in Table 4.

Please cite this article in press as: A. Rashkovska, et al., Non-invasive real-time prediction of inner knee temperatures during therapeutic cooling, Comput. Methods Programs Biomed. (2015), http://dx.doi.org/10.1016/j.cmpb.2015.07.004

from multiple runs for each pruning parameter. The scenarios are given in Table 4.

The models based on SC1, SC2, SC3 and SC4 are evaluated to investigate whether it is better to take more SK temperatures/sensors without history, or less SK temperatures/sensors with history as input attributes. First, SC1 and SC2 with all SK input attributes are evaluated and compared to investigate whether the predictive performance is better if the history of SK temperatures is taken as input attributes. Next, the SC3 and SC4 scenarios investigate if the reduction of SK temperatures as input attributes also gives satisfying predictive accuracy. Then, we compare the predictive performances of SC3 and SC5 in order to confirm the results from the feature ranking indicating that the temperatures on the bandage are not relevant for predicting the inner knee temperature. Finally, we validate the best performing model with real data from in vivo temperature measurement from a patient undergoing cryotherapy after ACL reconstruction.

4.2.1. *Evaluation of regression and model trees based on SC1 and SC2*

The results for the predictive performance and time/memory efficiency of the regression trees and model trees for SC1 and SC2 are presented in Fig. 3. The results show that the variations of the CC and MAE are very small for all pruning parameters, indicating stability of the models. The results for linear regression, ensembles of regression trees and ensembles of model trees are not shown on the graph because they do not perform well based on the system requirements. More precisely, the linear regression model does not have a satisfying predictive performance, even though the time/memory efficiency of such models is the best. The CC and MAE of the linear regression model are 0.7248 ± 0.001570 and 1.2249 ± 0.002494 for SC1, and 0.6541 ± 0.002117 and 1.2122 ± 0.004176 for SC2. The CC values for linear regression for both scenarios are far worse than the CC values for the regression and model trees, and the MAE values for linear regression for both scenarios are larger than 1 °C. On the other hand, the ensembles of regression and model trees have excellent predictive performances (MAE values typically smaller than 0.1 °C), but they do not perform in real-time – the memory/time efficiency does not satisfy the requirements. The size of the ensembles of regression and model trees is in the range of GB, which is unacceptable for small onboard computer architectures. Nevertheless, Fig. 3 shows that the regression trees and model trees perform very well and they comply with the system requirements.

The models based on SC1 have better predictive performance, showing that the inclusion of the history of the

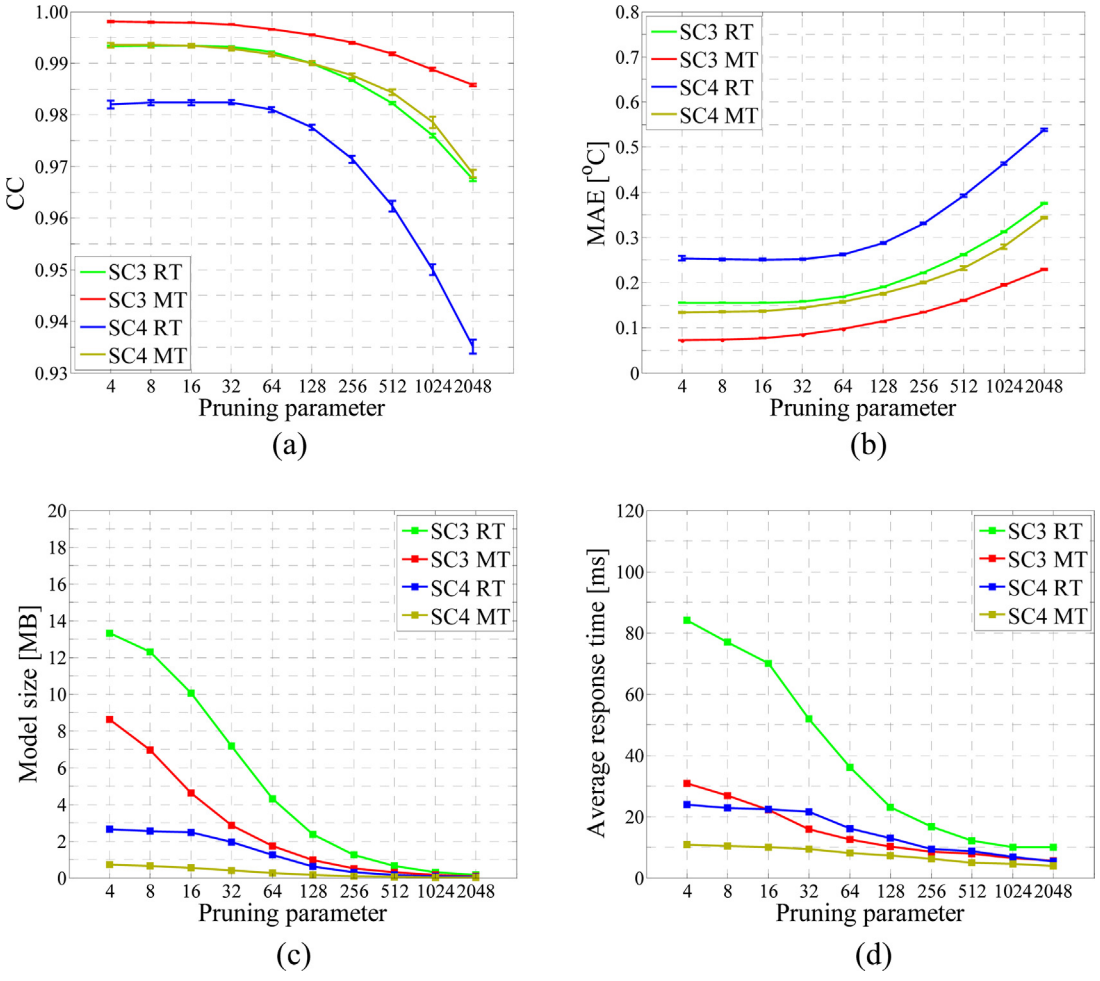

Fig. 4 – Performance of regression trees (RT) and model trees (MT) for SC3 and SC4 (a) correlation coefficient (CC), (b) mean absolute error (MAE), (c) model size and (d) time efficiency. SC3 and SC4 are defined in Table 4.

Please cite this article in press as: A. Rashkovska, et al., Non-invasive real-time prediction of inner knee temperatures during therapeutic cooling, Comput. Methods Programs Biomed. (2015), http://dx.doi.org/10.1016/j.cmpb.2015.07.004

knee temperature attributes improves the predictive accuracy. However, the models based on SC2 still have a satisfying predictive accuracy. The model trees for both scenarios perform better than the regression trees. The performance of the regression trees based on SC1 is similar to the one of the model trees based on SC2. More specifically, the model trees based on SC1 perform the best. The MAE of the model trees based on SC1 up until pruning parameter 32 are in the range of 0.1 °C, which is the accuracy of the simulated temperature data. We can use this information in order to lower the model size and not lose in performance. The decrease of the model size is due to the increase of the value for the pruning parameter, i.e., if we require more examples per leaf, then the trees will have fewer nodes. The size of the predictive models based on SC1 is bigger compared to SC2, but all models perform in real-time. The average response time is in the range of milliseconds for all models.

4.2.2. *Evaluation of regression and model trees based on SC3 and SC4*

The results for regression trees and model trees for SC3 and SC4 are presented in Fig. 4. Again, the results show that the variations of the CC and MAE for regression and model trees are very small for all pruning parameters. The results for linear regression, ensembles of regression trees and ensembles of model trees are also not presented. The same findings apply also here: they do not satisfy the requirements for predictive accuracy and real-time response. Namely, the CC and MAE of the linear regression model are 0.6935 ± 0.001157 and 1.1978 ± 0.001261 for SC3, and 0.6330 ± 0.005706 and 1.2258 ± 0.003825 for SC4.

The results for the regression trees and model trees show that the models perform well also with just two SK input attributes. Again, the predictive models based on SC3 with history of the SK1 and SK3 attributes perform better. Similarly, the model trees for both scenarios perform better than the regression trees. The model trees based on SC3 perform the best, with MAE still in the range of 0.1 °C up until pruning parameter 32. All models perform in real-time and have acceptable model size.

4.2.3. *Evaluation of models trees based on SC1, SC2, SC3 and SC4*

The results for all scenarios show that the model trees perform the best on the data resulting from the simulations. The simulation data based on the Bio-heat equation are piecewise linear, therefore the good performance of the model trees is understandable. Next, having established that the model trees perform the best, we compare the results for model trees for all scenarios. The comparison is presented in Fig. 5.

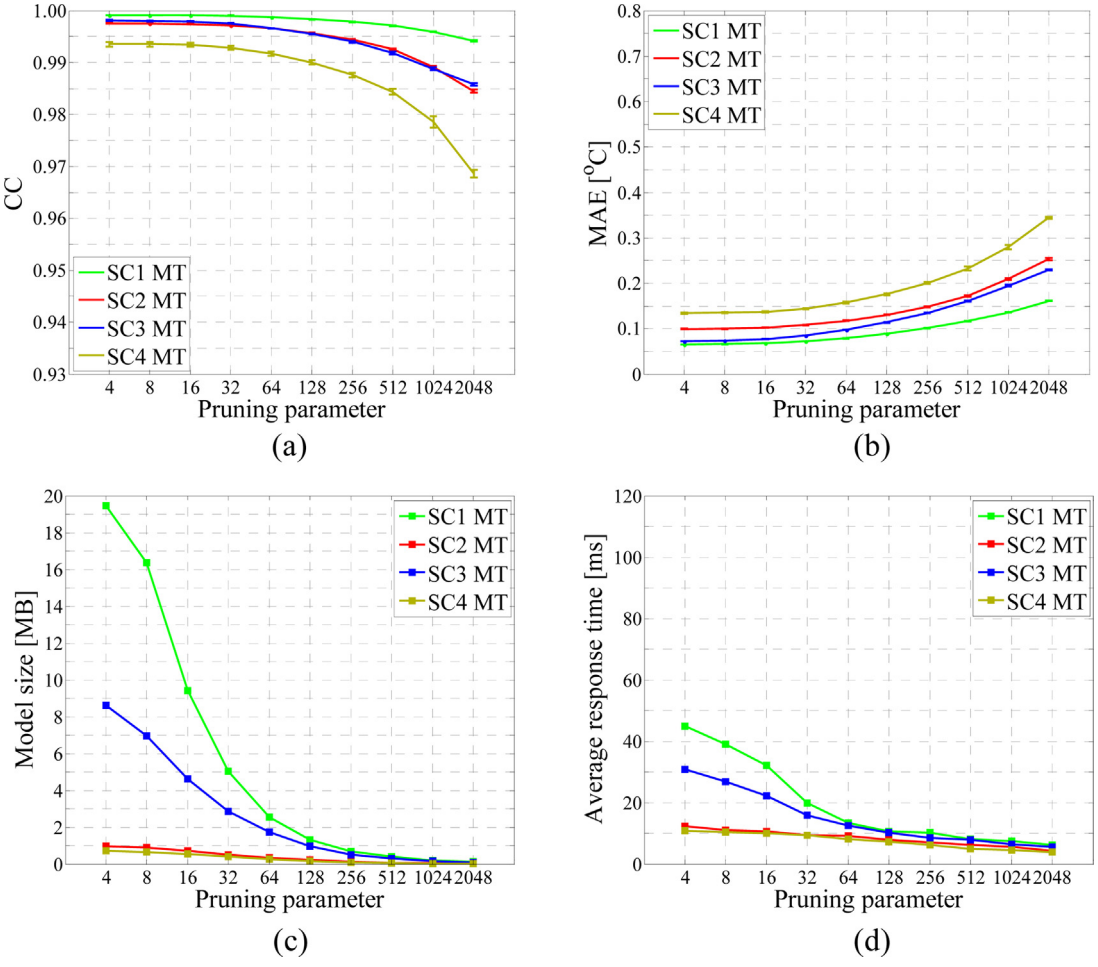

Fig. 5 – Performance of model trees (MT) for SC1, SC2, SC3 and SC4 (a) correlation coefficient (CC), (b) mean absolute error (MAE), (c) model size and (d) time efficiency. SC1, SC2, SC3 and SC4 are defined in Table 4.

Please cite this article in press as: A. Rashkovska, et al., Non-invasive real-time prediction of inner knee temperatures during therapeutic cooling, Comput. Methods Programs Biomed. (2015), http://dx.doi.org/10.1016/j.cmpb.2015.07.004

The results show that the model trees based on SC1 with history of all SK temperature attributes perform the best. However, the model trees based on SC3 with history for just two SK temperature attributes perform similar as the model tree based on SC2 with all SK temperature attributes without history. Hence, we can lower the number of SK temperature attributes/sensors from four to just two at the account of adding history in order to achieve the same performance. SC2 and SC4 construct smaller models with better time efficiency. If the request for smaller models must be met, the model for SC2 should be selected, as it shows better predictive performance.

4.2.4. *Evaluation of regression and models trees based on SC3 and SC5*

The feature ranking results from Table 3 indicate that the temperatures on the bandage are not relevant for predicting the inner knee temperature. We hypothesize that the bandage temperature is implicitly hidden in the skin temperature, and moreover in the cooling temperature of the pad. The cooling temperature provides enough information to the machine learning method without the bandage temperature. In order to test this hypothesis, we compare the predictive performances of SC3 and SC5. The set of input attributes of SC3 is complemented with BA1 temperature attributes to form SC5. BA1 attributes are tested because they are taken at a position above SK1 where the knee is most responsive to the changes in the cooling temperature. The results for the regression trees and model trees for SC3 and SC5 are compared in Fig. 6. The results clearly show that the performance of the models based on SC3 and SC5 is the same for all criteria, which confirms that additional third sensor on the bandage does not improve the predictive performance of the model. Moreover, the performances of the linear regression model for SC3 and SC5 are also very close, namely, the CC and MAE for the linear regression model are 0.6935 ± 0.001157 and 1.1978 ± 0.001261 for SC3, and 0.7039 ± 0.001574 and 1.1943 ± 0.002242 for SC5.

4.2.5. *Validation with real data*

The model tree based on SC2 has been validated also with real data. The in vivo measurements from the knee skin, obtained from a patient in the clinical study performed in Ref. [29], are the input attributes, while the in vivo measurement of the temperature in the intercondylar notch is the target. For the first interval of cooling at 9 °C, the measured and predicted temperatures in the intercondylar notch are shown in Fig. 7. The results show that the predicted temperature evolution for the cooling period shows good agreement with the measured values.

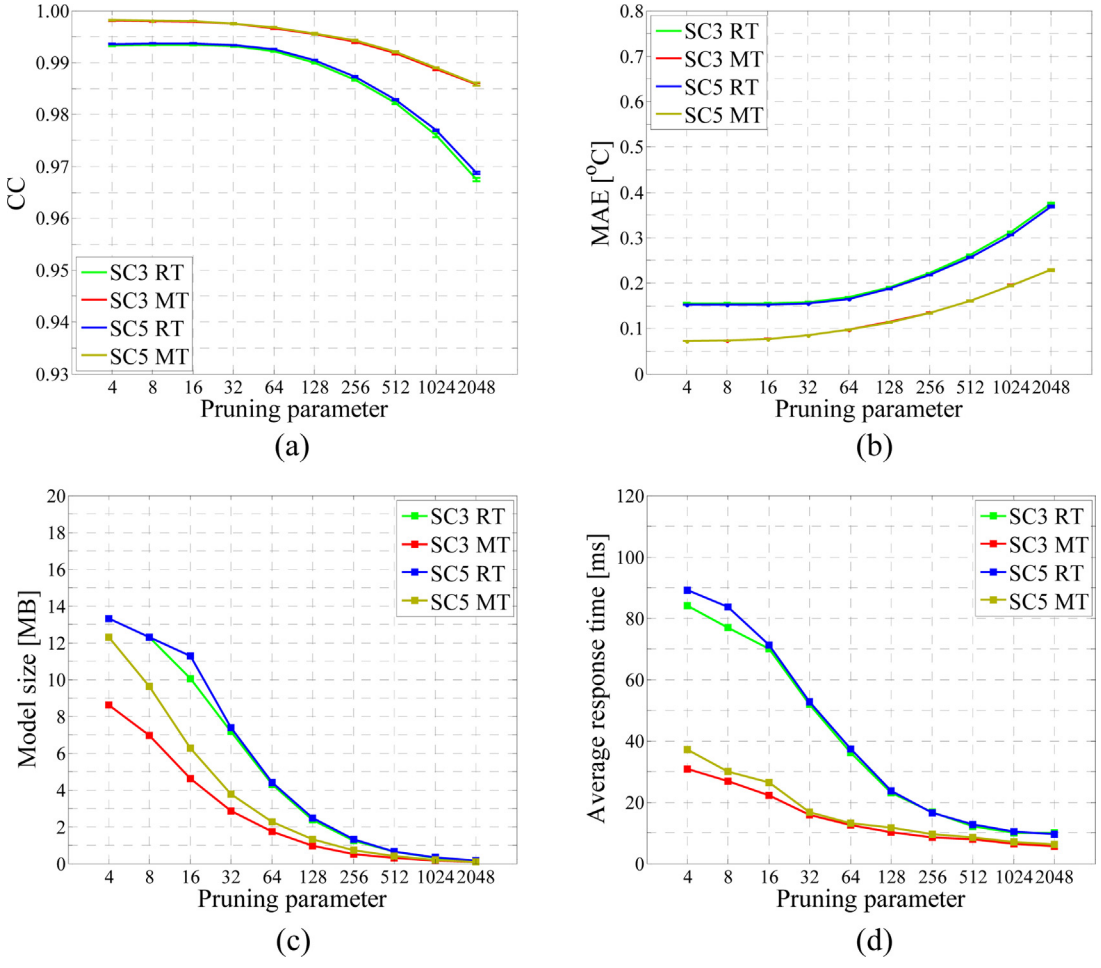

Fig. 6 – Performance of regression trees (RT) and model trees (MT) for SC3 and SC5 (a) correlation coefficient (CC), (b) mean absolute error (MAE), (c) model size and (d) time efficiency. SC3 and SC5 are defined in Table 4.

Please cite this article in press as: A. Rashkovska, et al., Non-invasive real-time prediction of inner knee temperatures during therapeutic cooling, Comput. Methods Programs Biomed. (2015), http://dx.doi.org/10.1016/j.cmpb.2015.07.004

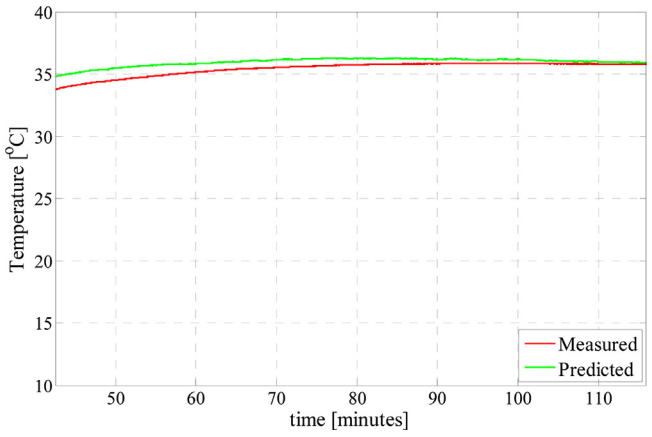

Fig. 7 – Measured vs. predicted temperature in the intercondylar notch. The predicted values are obtained with the model tree from SC2.

5. Conclusions

The paper implements and evaluates a method for real-time prediction of hidden variables during therapeutic cooling or heating where the inner body temperature cannot be measured either because the system is non-invasive, like most of the examples in biomedicine, or for any other reason. Therefore, other measurable variables of the system are used to estimate the hidden output variable of interest. The paper leverages two research areas from computer science and engineering for that purpose: computer simulations – to provide safe and inexpensive insight into the studied process/system, and machine learning – to provide methods for predicting the hidden output variable from the measurable ones based on the data generated from the simulations. The proposed approach is applied on a real-world problem in the domain of biomedicine – non-invasive real-time prediction of the inner knee temperature during cryotherapy after knee surgery.

Using the dataset from the simulated results, we have performed predictive modeling. First, feature ranking using the RReliefF method revealed that the most important features for predicting the inner knee temperature are the skin temperatures that correspond to the temperatures of skin sensors placed anterior and posterior to the knee. Based on the feature ranking results, we have investigated several scenarios for the performance of several methods for predictive modeling: linear regression, regression trees, model trees, and ensembles of regression and model trees. The model trees performed the best with prediction error in the same range as the accuracy of the simulated data (0.1 °C). Moreover, they satisfy the requirements for small memory size and real-time response. Results have shown that using only temperatures from skin sensors as input attributes gives excellent prediction for the temperature in the knee center. Moreover, satisfying predictive accuracy is also achieved using short history of temperatures from just two skin sensors (placed anterior and posterior to the knee) as input variables.

The need for non-invasive prediction of inner knee temperature during therapeutic cooling is based on the finding that the cryotherapy should be controlled depending on the individual patient's response [29], which raises the need for "smart" cooling devices for personalized therapy. Therefore, the proposed method for non-invasive prediction of inner knee temperature during therapeutic cooling can be included in a framework for real-time control of inner knee temperature based on the feedback control loop that uses predicted, instead of measured, inner temperatures because measurements are not feasible or would introduce invasiveness into the system [28].

The work presented in this paper can be extended in several directions. First, for achieving even better predictive performance in real-life therapeutic cooling, the dataset can be extended with simulated data for a wider range and/or higher resolution of already varied input parameters (cooling temperature, knee dimension and blood flow rate), or variations of other input simulation parameters. Next, the geometric model of the knee for the simulation can be personalized for each patient using, for example, the Magnetic Resonance Imaging (MRI) of the knee made before surgery. Finally, the proposed method for non-invasive real-time prediction of hidden inner body temperature variables can be applied for prediction of inner temperatures during therapeutic cooling or heating of any part of the body. The application includes using already developed valid simulation model of bio-heat transfer in the treated body part. The modular design and implementation allow for easy inclusion of different simulation or predictive models.

Acknowledgements

The authors Aleksandra Rashkovska and Roman Trobec acknowledge the financial support from the state budget by the Slovenian Research Agency under the grant P2-0095. Dragi Kocev is supported by the European Commission through the project MAESTRA – Learning from Massive, Incompletely annotated, and Structured Data (Grant number ICT-2013-612944).

REFERENCES

[1] M.J. Ackerman, The visible human project, Proc. IEEE 86 (1998) 505–511.
[2] P. Albertos, G.C. Goodwin, Virtual sensors for control applications, Annu. Rev. Control 26 (2002) 101–112.
[3] M. Antonic, B. Gersak, Renal function after port access and median sternotomy mitral valve surgery, Heart Surg. Forum (2007) E401–E407.
[4] P. Bernardi, M. Cavagnaro, S. Pisa, E. Piuzzi, Specific absorption rate and temperature elevation in a subject exposed in the far-field of radio-frequency sources operating in the 10-900-MHz range, IEEE Trans. Biomed. Eng. 50 (2003) 295–304.
[5] I. Bratko, I. Mozetič, N. Lavrač, KARDIO: A Study in Deep and Qualitative Knowledge for Expert Systems, MIT Press, Cambridge, MA, 1989.
[6] L. Breiman, Bagging predictors, Mach. Learn. 24 (1996) 123–140.
[7] L. Breiman, J.H. Friedman, R.A. Olshen, C.J. Stone, Classification and Regression Trees, Wadsworth, Belmont, CA, 1984.

[8] C.K. Charny, Mathematical models of bioheat transfer, in: Advances in Heat Transfer, Academic Press, New York, 1992.
[9] O. Chertov, et al., Geovizualization of forest simulation modelling results: a case study of carbon sequestration and biodiversity, ACM Trans. Math. Softw. 49 (2005) 175–191.
[10] N. Filipovic, M. Ivanovic, D. Krstajic, M. Kojic, Hemodynamic flow modeling through an abdominal aorta aneurysm using data mining tools, IEEE Trans. Inf. Technol. Biomed. 15 (2011) 189–194.
[11] W.A. Grana, Cold modalities, in: J.C. DeLee, D. Drez (Eds.), Orthopaedic Sports Medicine, Principles and Practice, WB Saunders, Philadelphia, PA, USA, 1994.
[12] T. Hastie, R. Tibshirani, J. Friedman, The Elements of Statistical Learning, Springer, 2001.
[13] M.T. Heath, Scientific Computing: An Introductory Survey, 2nd ed., McGraw-Hill, New York, 2002.
[14] S.S. Ho, M.N. Coel, R. Kagawa, A. Richardson, The effects of ice on blood flow and bone metabolism in knees, Am. J. Sports Med. 22 (1994) 537–540.
[15] B. Karaszewski, et al., Measurement of brain temperature with magnetic resonance spectroscopy in acute ischemic stroke, Ann. Neurol. 60 (2006) 438–446.
[16] I. Kononenko, M. Kukar, Machine Learning and Data Mining: Introduction to Principles and Algorithms, Woodhead Publishing, Chichester, West Sussex, 2007.
[17] P. Langley, Elements of Machine Learning, Morgan Kaufmann Publishers Inc., San Francisco, CA, USA, 1996.
[18] R.L. Martino, C.A. Johnson, E.B. Suh, Parallel computing in biomedical research, Science 265 (1994) 902–908.
[19] S.S. Martin, K.P. Spindler, J.W. Tarter, K. Detwiler, H.A. Petersen, Cryotherapy: an effective modality for decreasing intraarticular temperature after knee arthroscopy, Am. J. Sports Med. 29 (2001) 288–291.
[20] T. Mitchell, Machine Learning, McGraw Hill, 1997.
[21] D. Mladenič, I. Bratko, R.J. Paul, M. Grobelnik, Using machine learning techniques to interpret results from discrete event simulation, in: Proceedings from ECML '94: The European Conference on Machine Learning, Secaucus, NJ, 1994, pp. 399–402.
[22] E.Y.K. Ng, L.T. Chua, Prediction of skin burn injury. Part 1: Numerical modelling, in: Proc. Inst. Mech. Eng. H. Journal of Engineering in Medicine 216 (March (3)), 2002, pp. 157–170.
[23] E.Y.K. Ng, L.T. Chua, Prediction of skin burn injury. Part 2: Parametric and sensitivity analysis, in: Proc. Inst. Mech. Eng. H. Journal of Engineering in Medicine 216 (March (3)), 2002, pp. 171–183.
[24] E.Y.K. Ng, H.M. Tan, E.H. Ooi, Prediction and parametric analysis of thermal profiles within heated human skin using the boundary element method, Philos. Trans. Ser. A Math. Phys. Eng. Sci. 368 (February (1912)) (2010) 655–678.
[25] M.N. Őzisik, Finite Difference Methods in Heat Transfer, CRC Press, Boca Raton, 2000.
[26] H.H. Pennes, Analysis of tissue and arterial blood temperature in the resting human forearm, J. Appl. Physiol. 1 (1948) 93–122.
[27] R.J. Quinlan, Learning with continuous classes, in: Proceedings from AI '92: The Fifth Australian Joint Conference on Artificial Intelligence, Singapore, 1992, pp. 343–348.
[28] A. Rashkovska, R. Trobec, Method and device for non-invasive real-time control of inner body temperature variables during therapeutic cooling or heating, 2013.
[29] A. Rashkovska, R. Trobec, V. Avbelj, M. Veselko, Knee temperatures measured in vivo after arthroscopic ACL reconstruction followed by cryotherapy with gel-packs or computer controlled heat extraction, Knee Surg. Sports Traumato. Arthrosc. (2013).
[30] A. Rashkovska, R. Trobec, M. Depolli, G. Kosec, 3D numerical simulation of heat transfer in biomedical applications, in: S.N. Kazi (Ed.), Heat Transfer Phenomena and Applications, InTech, Rijeka, 2012, pp. 99–151.
[31] R.C. Richie, Non-invasive assessment of the risk of coronary heart disease, J. Insur. Med. 34 (2002) 31–42.
[32] M. Robnik-Šikonja, I. Kononenko, An adaptation of Relief for attribute estimation in regression, in: Proceedings from ICML '97: The Fourteenth International Conference on Machine Learning, San Francisco, CA, 1997, pp. 296–304.
[33] M. Robnik-Šikonja, I. Kononenko, Theoretical and empirical analysis of ReliefF and RReliefF, Mach. Learn. J. 53 (2003) 23–69.
[34] M. Rohrscheib, R. Robinson, R.P. Eaton, Non-invasive glucose sensors and improved informatics – the future of diabetes management, Diabetes Obes. Metab. 5 (2003) 280–284.
[35] H.J. Schaubel, The local use of ice after orthopedic procedures, Am. J. Surg. 72 (1946) 711–714.
[36] G. Seni, J.F. Elder, Ensemble Methods in Data Mining: Improving Accuracy Through Combining Predictions, Morgan & Claypool Publishers, San Rafael, CA, 2010.
[37] D.H. Silverthorn, Human Physiology, An Integrated Approach, Prentice-Hall, New Jersey, 2001.
[38] M. Šterk, R. Trobec, Biomedical simulation of heat transfer in a human heart, J. Chem. Inf. Model. 45 (2005) 1558–1563.
[39] H. Sugimoto, W.W. Monafo, Regional blood flow in sciatic nerve, biceps femoris muscle, and truncal skin in response to hemorrhagic hypotension, J. Trauma 27 (1987) 1025–1030.
[40] K. Tachibana, Emerging technologies in therapeutic ultrasound: thermal ablation to gene delivery, Hum. Cell 17 (2004) 7–15.
[41] P. Tikuisis, M.B. Ducharme, Finite-element solution of thermal conductivity of muscle during cold water immersion, J. Appl. Physiol. 70 (1991) 2673–2681.
[42] R. Trobec, Parallel computer simulations of heat transfer in biological tissues, in: R. Trobec, M. Vajteršic, P. Zinterhof (Eds.), Parallel Computing: Numerics, Applications, and Trends, Springer, Dordrecht, Netherlands, 2009, pp. 307–358.
[43] R. Trobec, M. Depolli, Simulated temperature distribution of the proximal forearm, Comput. Biol. Med. 41 (2011) 971–979.
[44] R. Trobec, B. Slivnik, B. Geršak, T. Gabrijelčič, Computer simulation and spatial modelling in heart surgery, Comput. Biol. Med. 28 (1998) 393–403.
[45] R. Trobec, M. Šterk, S. Almawed, M. Veselko, Computer simulation of topical knee cooling, Comput. Biol. Med. 38 (2008) 1076–1083.
[46] P. Trunk, B. Geršak, R. Trobec, Topical cardiac cooling – computer simulation of myocardial temperature changes, Comput. Biol. Med. 33 (2003) 203–214.
[47] Waegener R&D, Belgium, http://www.waegener.com
[48] E.H. Wissler, Pennes' 1948 paper revisited, J. Appl. Physiol. 85 (1998) 35–41.
[49] I.H. Witten, E. Frank, Data Mining: Practical Machine Learning Tools and Techniques, Morgan Kaufmann, San Francisco, CA, 2005.
[50] F. Xu, T.J. Lu, K.A. Seffen, E.Y.K. Ng, Mathematical modeling of skin bioheat transfer, Appl. Mech. Rev. 62 (July (5)) (2009).
[51] F. Yamazaki, R. Sone, Modulation of arterial baroreflex control of heart rate by skin cooling and heating in humans, J. Appl. Physiol. 88 (2000) 393–400.

Please cite this article in press as: A. Rashkovska, et al., Non-invasive real-time prediction of inner knee temperatures during therapeutic cooling, Comput. Methods Programs Biomed. (2015), http://dx.doi.org/10.1016/j.cmpb.2015.07.004